Aerosol and Air Quality Research

ORIGINAL RESEARCH
https://doi.org/10.4209/aaqr.210333

Variations in Sources, Composition, and Exposure Risks of $PM_{2.5}$ in both Pre-Heating and Heating Seasons

Dingyuan Yang[1], Zhiyong Li[1,2*], Ziyuan Yue[1], Jixiang Liu[1], Zhen Zhai[1], Zelin Li[1], Minglei Gao[1], Ailian Hu[1], Wenjia Zhu[1], Ning Ding[1], Zhenxin Li[1], Songtao Guo[1], Xiangxue Wang[1,2], Lei Wang[3*], Jihong Wei[4]

[1] Hebei Key Lab of Power Plant Flue Gas Multi-Pollutants Control, Department of Environmental Science and Engineering, North China Electric Power University, Baoding 071003, China
[2] MOE Key Laboratory of Resources and Environmental Systems Optimization, College of Environmental Science and Engineering, North China Electric Power University, Beijing 102206, China
[3] Hebei Research Center for Geoanalysis, Baoding 071003, China
[4] Department of Pediatrics, Affiliated Hospital of Hebei University, Baoding 071000, China

ABSTRACT

"Clean Heating" (CH) was promoted in 2017 in north China. Nevertheless, CH impacts on $PM_{2.5}$ chemical components, sources, and health risks in small cities remain unclear. A field measurement was taken at an urban site within the central Beijing-Tianjin-Hebei (BTH) region covering the pre-heating season (PHS) and heating season (HS) in the winter of 2019. $PM_{2.5}$ concentrations (in μg m^{-3}) increased from 69.1 in the PHS to 129 in the HS, reflecting the impacts of heating activities. Water-soluble ions dominated in terms of $PM_{2.5}$, accounting for 32.0% in the PHS and 42.3% in the HS, respectively. On average, SO_4^{2-} and NO_3^- (in μg m^{-3}) were found to be markedly enhanced from 3.54 and 11.1 in the PHS to 13.1 and 23.2 in the HS, especially in the case of SO_4^{2-}, reflecting the increased usage of coal/natural gas. Meanwhile, the ratios of NO_3^-/SO_4^{2-} dropped from 2.75 in the PHS to 2.08 in the HS, implying drastic SO_4^{2-} emissions from coal combustion used for heating. This may have been associated with the re-burning of coal for heating despite the "coal banning" law. Total carcinogenic risks (CRs) posed by inhalation of heavy metals increased from 6.61×10^{-6} in children and 2.64×10^{-5} in adults in the PHS to 8.23×10^{-6} and 3.29×10^{-5} in the HS. In contrast, the non-CRs for children and adults decreased in the HS due to a reduction in Ba of 85.5% in the HS. A total of seven sources, including fugitive dust (FD), vehicle exhaust (VE), coal combustion (CC), secondary inorganic aerosol (SIA), industrial emissions (IE), glass production (GP), and biomass burning (BB), were identified using a PMF model. The GP fraction decreased from 29.6% in the PHS to 2.59% in the HS due to strict emission control, which concurred with the decrease in Ba. The CC contribution increased significantly from 2.42% to 16.9%, indicating the CC was still serious in HS. Furthermore, the elevated BB share in the HS suggested that biomass was still being used as heating fuel.

Keywords: $PM_{2.5}$, Source apportionment, Clean heating, Health risk, Heavy metal

OPEN ACCESS

Received: December 6, 2021
Revised: January 15, 2022
Accepted: January 16, 2022

* **Corresponding Authors:**
Zhiyong Li
lzy6566@126.com
Lei Wang
wanglei8812@126.com

Publisher:
Taiwan Association for Aerosol Research
ISSN: 1680-8584 print
ISSN: 2071-1409 online

1 INTRODUCTION

The Beijing-Tianjin-Hebei (BTH) region, the center of the North China Plain, has suffered from severe pollution due to fine particulate matter ($PM_{2.5}$, an aerodynamic diameter less than or equal to 2.5 μm), especially in the heating season (Cheng *et al.*, 2019; Zhai *et al.*, 2019; Li *et al.*, 2020a, b, 2021a, b). $PM_{2.5}$ mainly includes water-soluble ions, trace elements, organic carbon, elemental carbon, and dust, all of which have adverse effects on the climate and human health

(Li *et al.*, 2020a, b; Wang *et al.*, 2021). To mitigate this crisis in the BTH, the Chinese government issued an "Atmospheric Pollution Prevention Plan" (Clean Air Action) in 2013, which was aimed toward markedly reducing $PM_{2.5}$ by 25% by 2017 (Chen *et al.*, 2019). However, $PM_{2.5}$ was still at a high level in the BTH region regardless of this 20% reduction in the peak $PM_{2.5}$, which was attributed to the migration of air pollutants from other regions, especially during the heating season (Zheng *et al.*, 2018). Airborne pollutant transport between neighboring cities also resulted in high $PM_{2.5}$ levels in Beijing, and regional integration has proven to be one of main solutions to mitigate this crisis (Chen *et al.*, 2019). Therefore, a "2 + 26" strategy covering Beijing, Tianjin, and 26 other cities acting as an "air pollution transmission channel" in four neighboring northern provinces (Hebei, Henan, Shandong, and Shanxi) was promoted by the Ministry of Ecology and Environment to further improve the air quality in Beijing and the BTH region during heating season (Chen *et al.*, 2019).

As a key part of "2 + 26" policy, clean heating (CH) was vigorously promoted in the winter of 2017 (Chen *et al.*, 2019; Cheng *et al.*, 2019). Strengthening the management of raw coal in rural areas, eliminating backward coal-fired boilers, shutting down small scale coal-related enterprises, and developing central heating for cities with more than 200,000 residents were all parts of the CH policy (http://www.mee.gov.cn/gkml/hbb/bwj/201708/t20170824_420330.htm). As a result, $PM_{2.5}$ decreased markedly, and its chemical composition was notably altered (Zhai *et al.*, 2019). Long-term monitoring of 338 cities indicated an overall improvement in air quality along with a noticeable 33% reduction in $PM_{2.5}$ and a 59% reduction in SO_2 (Zheng *et al.*, 2018). However, undesirable outcomes included dramatically elevated O_3, NH_3, and VOCs, accompanied with stagnant or elevated NO_x, were found in North China (Zhai *et al.*, 2019). Nitrate formation promoted by the stagnant NO_x and enhanced NH_3 offset the present decrease in $PM_{2.5}$ due to a reduction in SO_2, and the relationship between severe pollution events and nitrate became more apparent (Xu *et al.*, 2019). The disparity between the still high $PM_{2.5}$ and the air quality standard in the BTH region, especially during heating season, was the main obstacle to substantially improving air quality (Zhai *et al.*, 2019).

Effective implementation of the CH policy was largely dependent on the acknowledgement of provision of $PM_{2.5}$ data compliance with policies in small cities (Carter *et al.*, 2020). Most of the "2+26" cities are small cities; therefore, it was necessary to understand the differences in $PM_{2.5}$ sources, composition, and exposure risk between the PHS and the HS. However, current studies have mainly focused on large metropolitan areas, urban agglomerations, and rural areas (Chen *et al.*, 2019; Zhao *et al.*, 2020a, b).

In this study, intensive observation was carried out covering both the PHS (October 25–November 14, 2019) and the HS (November 15, 2019–January 15, 2020) in Baoding. The main purposes of this study were to (1) investigate changes in the chemical composition of $PM_{2.5}$ in the HS, (2) evaluate differences in health risk related to exposure to heavy metals between the PHS and the HS, and (3) assess changes in source contributions of $PM_{2.5}$ from the PHS to the HS.

2 METHODOLOGY

2.1 Site Description

Baoding is positioned in the center of the Beijing-Tianjin-Hebei (BTH) region (Fig. 1). Baoding covers 22,190 km^2 and has a permanent population of 9,390,000. $PM_{2.5}$ was collected in a typical residential area with instruments were installed on the roof of an office building (30 m above ground) at North China Electric Power University (38°88'N; 115°51'E). The site is surrounded by residential buildings within a 3.5 km radius and therefore can be categorized as a typical residential zone.

2.2 $PM_{2.5}$ Sampling

$PM_{2.5}$ samples were simultaneously collected using two medium-volume air samplers (TH-150C, Wuhan Tianhong Instrument Co., Ltd.) with a flow rate of 100 L min^{-1}. Two kinds of filters, including a 90 mm quartz fiber (QF) filter (Pall USA) and a 90 mm Teflon (PTEE) filter (Whatman UK) were used. The sampling lasted for approximately 23 h (10:00 AM–9:00 AM of the next day). Field blanks were used every 8 samples, and a total of 64 samples and 7 blanks were obtained.

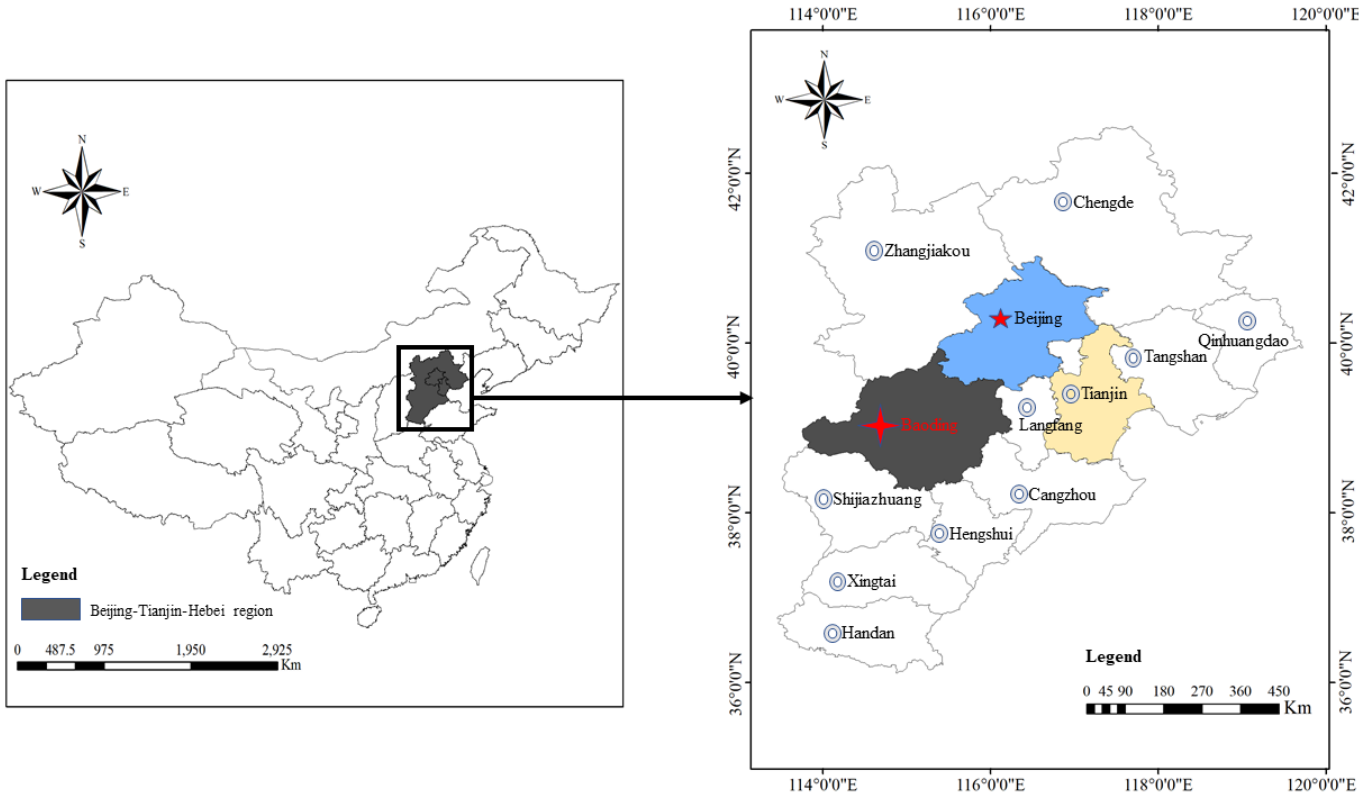

Fig. 1. Location of sampling point in Baoding City.

The QF filters were pre-heated at 800°C for 3 h before sample collection. The filters were stored in a room at a constant temperature (20°C) and relative humidity (50%) before and after sampling for the purpose of weighing. The filters were weighed gravimetrically using a Sartorius ME-5F microbalance with a sensitivity of ±1 μg (Sartorius, Göttingen, Germany). Each filter was weighed at least three times before and after sampling. Deviations among replicate weights were mostly lower than 15 μg for each filter. Net mass was acquired by subtracting the pre-weight from the post-weight. The samples were stored in a freezer at –20°C prior to analysis.

2.3 Chemical Analysis

Each PTEE filter was cut into two equal halves and analyzed for 39 elements and 9 water-soluble ions (WSIs), respectively. The two halves underwent different digestion procedures for the analysis of 30 elements (Li, Be, Na, P, K, Sc, V, Cr, Mn, Co, Ni, Cu, Zn, As, Rb, Y, Mo, Cd, Sn, Sb, Cs, La, Ce, Sm, W, Tl, Pb, Bi, Ti, and Th) with the ICP-MS system (Agilent 7500a, USA) and 9 elements (Al, Ca, Mg, Fe, Ba, Sr, Zr, Si, and U) with the ICP-OES system (Agilent 5100, USA), respectively. For the ICP-MS, one half of the PTEE was digested using an acid mixture (aqua regia/HF) at 120°C for 2 h and then dried at 130°C. It was finally heated with HCl and held for measurement. For ICP-OES, another half was ashed at 550°C, mixed with absolute ethanol and NaOH and boiled with water. Finally, the solution was analyzed using the ICP-OES system. The same procedures were adopted for one regent blank and three filter blanks. The instrument calibration was conducted using a multi-element standard (GBW7446–7457) purchased from the Chinese Center for National Standard Material Center. The recoveries for all the elements fell within ± 10% of the certified values. Calibration was carried out with multi-element standards (GBW07446–07457). Precision for most elements were better than 5% (n = 5). Additional information about the QA/QC and analytical procedures can be found in Tao *et al.* (2014) and Li *et al.* (2021b).

One half of the QF filter was used for the WSI analysis and detailed as described in Li *et al.* (2021b). It was ultrasonically extracted for 20 mins at least three times. The extracts were subsequently passed through a microporous membrane with a pore size of 0.22 μm (Whatman, Middlesex, UK), put into a plastic bottle, and held at 4°C prior to analysis. The 4 anions (SO_4^{2-}, NO_3^-, Cl^-, and F^-)

and 4 cations (K^+, Na^+, Ca^{2+}, and Mg^{2+}) were analyzed using the ICS-1000 system (Thermo Scientific, USA) and the ICP-OES system (Agilent 725, Agilent Co. USA), respectively, with the method detection limits (MDLs) were 0.005–0.013 μg mL^{-1} and 0.002–0.025 μg mL^{-1}, respectively. An ultraviolet-visible spectrophotometer (UV-VIS, T6, Beijing General Instruments Co., Ltd.) was employed to measure the remaining NH_4^+ and the MDL was 0.002 μg mL^{-1}. The recoveries for all the 9 WSIs were within 100 ± 20%.

2.4 Backward Trajectory Clustering

Backward trajectory clustering is a tool widely applied to evaluate the origins of pollutant-containing air masses at receptor locations (Xu *et al.*, 2019). Three-dimensional backward trajectories were calculated using the Hybrid Single-Particle Lagrangian Integrated Trajectory model (HYSPLIT-4, http://ready.arl.noaa.gov/HYSPLIT.php) at elevations of 500 m and 1500 m.

2.5 Health Risk Assessment

In this study, health risks posed by the inhalation of heavy metals were selected to represent total risks (Si *et al.*, 2021). As, Cd, Cr(VI), Ni, Pb and Co were utilized to evaluate carcinogenic risks (CRs). Meanwhile, As, Cr, Ni, Pb, Co, Fe, Cu, Zn, Cd, Sb, Mn, Sr, Sn, Ba and Tl were examined in the non-cancer risk (NCR) assessment. A seventh of the total Cr was used to represent Cr(VI) (Mejido *et al.*, 2017). NCRs were presented as hazard quotients (HQs) (Si *et al.*, 2021). According to the regulatory purposes, *the* acceptable or tolerable risk was 1×10^{-6}–1×10^{-4} for CR, and a risk lower than 1 was used for the HQ (Si *et al.*, 2021).

In this study, we used the risk assessment model recommended by the US EPA to evaluate the risks posed by inhalation of $PM_{2.5}$-associated heavy metals (Megido *et al.*, 2017). The exposure concentration by inhalation (EC_{inh} (μg m^{-3})) was estimated using Eq. (1).

$$EC_{inh} = C \cdot ET \cdot \frac{EF \cdot ED}{AT_n} \tag{1}$$

where EC_{inh} is the exposure concentration (μg m^{-3}); C is the 95% upper confidence limit (UCL) on the arithmetic mean, representing the "reasonable maximum exposure" in the exposure assessment; ET is the exposure time (24 h day^{-1}); EF is the exposure frequency (day $year^{-1}$); ED is the exposure duration (year), and AT_n is the average time (day).

The CRs posed by inhalation were further calculated following the formula, where IUR represented the inhalation unit risk ((μg m^{-3}) $^{-1}$).

$$CR_{inh} = IUR \tag{2}$$

HQ_{inh} derived from inhalation of heavy metals was obtained using the following equation (Megido *et al.*, 2017; Si *et al.*, 2021), where the RfDo is the oral reference dose (mg kg^{-1} day^{-1}).

$$HQ_{ing} = \frac{CDI_{ing}}{RfDo} \tag{3}$$

$$HI = \sum HQ_i \tag{4}$$

All the parameters are illustrated in detail in Hu *et al.* (2012) and Mejido *et al.* (2017) and are listed in Table S1.

2.6 Source Apportionment of $PM_{2.5}$ by PMF

PMF was a multivariate factor analysis tool based on non-negative constraints used to obtain realistic factors (Tao *et al.*, 2014; Si *et al.*, 2021). Unlike principal component analysis (PCA) and chemical mass balance (CMB) models, the negative factor loadings could be eliminated, and the source spectrum was not needed in the PMF run (Lang *et al.*, 2018). The EPA PMF 5.0 program was used for the receptor modeling in this work. The uncertainty was calculated as follows:

For $c_i \leq$ MDL, unc = 5/6 × MDL (5)

For $c_i \geq$ MDL, unc = $[(c_i/5)^2 + MDL^2]^{0.5}$ (6)

The half MDL was used to represent the corresponding mass content below the MDL. The geometric mean of the observed values was used to replace the missing values, and the 4 times of the geometric mean indicated their uncertainty (Zhang *et al.*, 2018).

3 RESULTS AND DISCUSSION

3.1 $PM_{2.5}$ Concentration

The daily average $PM_{2.5}$ concentrations fluctuated from 14.6 to 232 μg m^{-3}, with a mean value of 110 μg m^{-3} (Fig. S1). The mean $PM_{2.5}$ increased significantly from 69.1 in the PHS to 129 μg m^{-3} in the HS. The higher $PM_{2.5}$ in the HS indicated strong heating effects, which was in agreement with findings suggesting this frequently occurs in north China in the HS (Zhang *et al.*, 2018; Zhai *et al.*, 2019). Despite the "coal banning" law, some rural areas in Hebei Province still use coal as a main energy source for heating, causing an elevation of $PM_{2.5}$ (Pang *et al.*, 2020). Furthermore, as high as 91.1% of sampling days showed a daily $PM_{2.5}$ value of more than 75 μg m^{-3} assigned as Chinese National Ambient Air Quality Standard Grade II. A previous study reported that $PM_{2.5}$ decreased by 71.2% in 2017 as compared with 2016 in Baoding City due to the "Coal to Gas" (CTG) policy in 2017 (Si *et al.*, 2021). The increase in $PM_{2.5}$ in this study compared with that in 2017 implied that coal usage may have increased due to laxity related to the CTG policy implementation. Meanwhile, the mean $PM_{2.5}$ in Baoding in the HS was much higher than the 94.5 μg m^{-3} found for Beijing, 111 μg m^{-3} for Tianjin, and 106 μg m^{-3} for Langfang in 2016–2017 (Pang *et al.*, 2020).

3.2 Concentrations of Water-soluble Ions (WSIs)

The daily total WSIs had an average of 47.0 μg m^{-3}, constituting 42.6% of the $PM_{2.5}$ mass. NO_3^-, NH_4^+, SO_4^{2-}, Ca^{2+}, and Cl^- were the predominant ions, contributing 41.3%, 23.1%, 21.5%, 15.3%, and 8.29% to the total WSIs, respectively (Fig. 2 and Table S2). Like the results reported recently in north China, NO_3^- increased along with the CTG policy and became the highest ion in the HS (Zhai *et al.*, 2019). 91% of the sampling days with $PM_{2.5}$ values higher than 75 μg m^{-3} were closely related to high NO_3^- (Huang *et al.*, 2021). The mass concentrations of NO_3^-, NH_4^+, SO_4^{2-}, and Cl^-

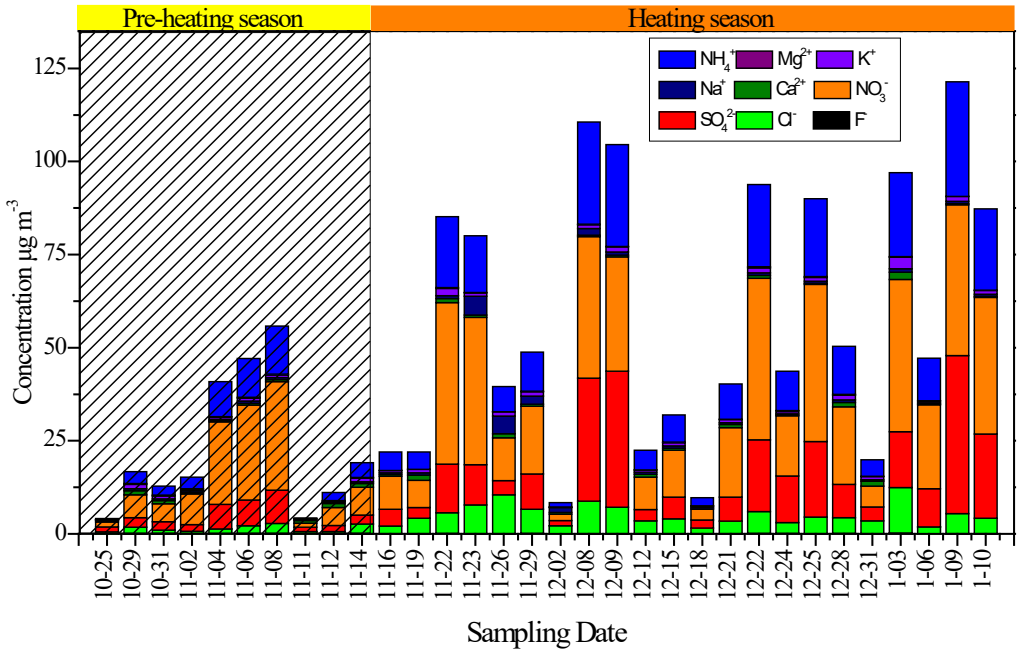

Fig. 2. Time series of water-soluble ion species.

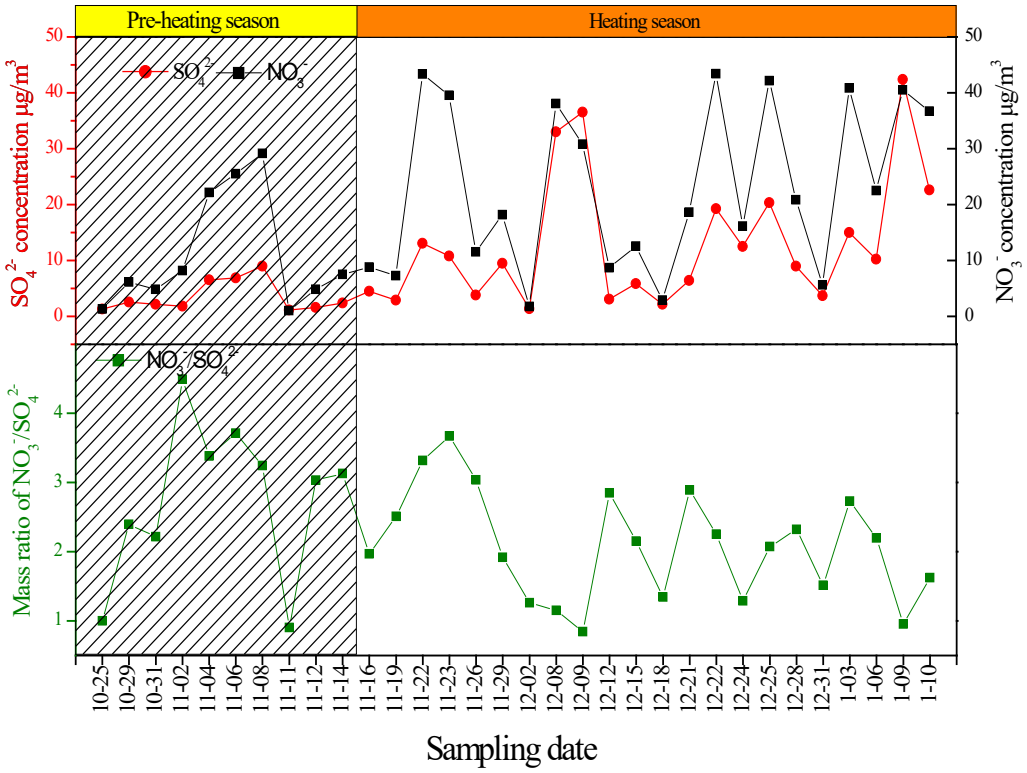

Fig. 3. Time series of concentrations of SO_4^{2-}, NO_3^-, and mass ratios of NO_3^-/SO_4^{2-}.

went up to 19.4, 10.8, 10.1, and 3.89 μg m^{-3} in the HS. The total SO_4^{2-}, NO_3^-, and NH_4^+ (SNN) contributed 80.4% and 32.6% to the entire WSIs and $PM_{2.5}$ for Baoding in the HS.

The mass ratio of NO_3^-/SO_4^{2-} (N/S) was a distinct indicator used to identify the relative importance of the coal combustion sources and vehicular sources (Tao *et al.*, 2014; Si *et al.*, 2021). Fig. 3 illustrates a time series of the concentrations of SO_4^{2-} and NO_3^- and the N/S ratios. Both SO_4^{2-} and NO_3^- increased significantly along with the transition from the PHS to the HS. On average, SO_4^{2-} and NO_3^- (in μg m^{-3}) varied from 1.16 to 8.98 and from 1.05 to 29.1 in the PHS, and from 1.38 to 42.4 and from 1.73 to 43.4 in the HS. A high N/S ratio of 2.29 during the entire sampling period (ESP) in Baoding suggested the CTG impacts the emissions of SO_4^{2-} and NO_3^- (Pozzer *et al.*, 2020). The N/S ratios in Baoding were much higher than 0.95 in 2016 for Shijiazhuang (Lang *et al.*, 2018), and 1.28 for the background site in the North China Plain (Yao *et al.*, 2016).

Previous studies have found more enhanced N/S ratios in the HS as compared to in the PHS in north China due to the sharp decrease in SO_4^{2-} due to the CTG project and coal banning law (Chen *et al.*, 2019; Zhai *et al.*, 2019; Li *et al.*, 2020). It should be noted that the decreased N/S from 2.75 in the PHS to 2.08 in the HS might have been related to the revival of coal-burning for heating purposes. This suggestion was in good agreement with the fact some rural residents began to reuse coal as heating fuel driven by lower costs (Carter *et al.*, 2020).

3.3 Trace Element Oxides and Soil Dust

The $PM_{2.5}$ mass was reconstructed as the total inorganic components (SNA: sulfate, nitrate, and ammonium), EC, dust, trace elements oxides (TEO), organic matter (OM). Si, Ca, Al, Fe, and Ti were used to calculate the soil dust (SD) based on [SD] = 1.89 × [Al] + 2.14 × [Si] + 1.4 × [Ca] + 1.43 × [Fe] + 1.66 × [Mg] + 1.67 × [Ti]. TEO was evaluated using TEO = 1.3 × [0.5 × (Sr + Ba + Mn + Co + Rb + Ni + V) + 1.0 × (Cu + Zn + Mo + Cd + Sn + Sb + Tl + Pb + As + Se + Ge + Cs + Ga)] (Tao *et al.*, 2014). Because of the lack of Se, Ge and Ga, the TEO was slightly underestimated. Fig. 4 shows the TEO and SD concentrations in winter in Baoding.

From the PHS to the HS, the SD fractions obviously declined from 19.8% to 7.81% due to control of fugitive dust and the low wind speed in the HS. A small variability was found for TEO, decreasing

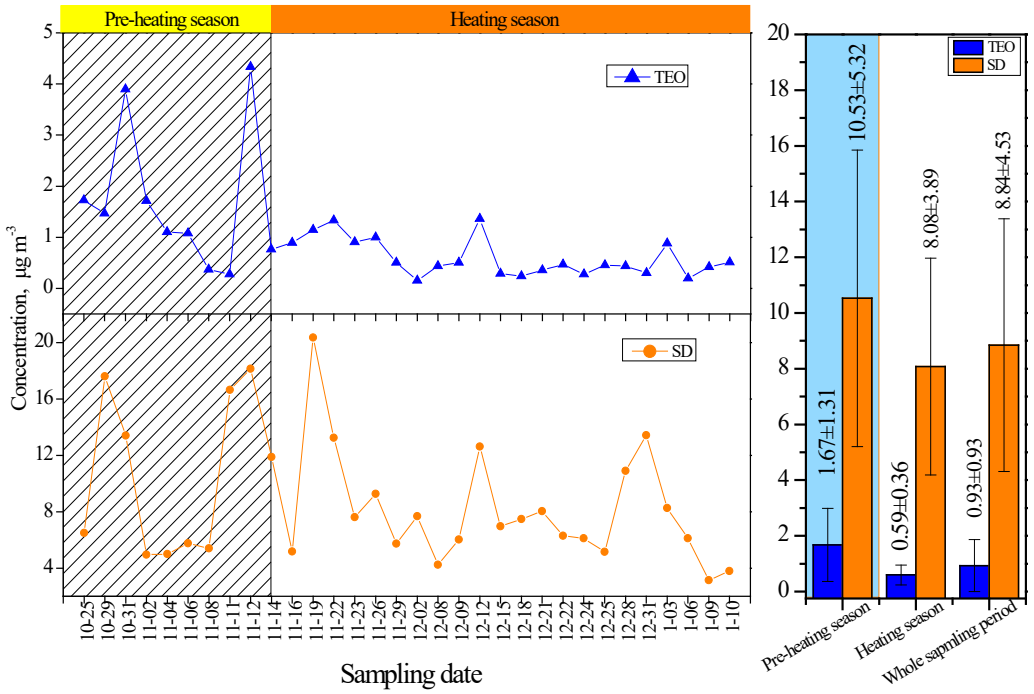

Fig. 4. Mass contents of trace element oxides and soil dust for each day, the pre-heating season, and the heating season.

from 3.47% to 0.53%. The decreased TEO fractions were attributed to emissions control on related industries in the heating season. SD fractions in both the PHS and HS were higher than 6.3% in Chengdu (Tao *et al.*, 2014), which suggested a strong impact of fugitive dust in North China. The decreased TEO in the HS was mainly attributed to the emission reductions in industrial processes when increases in heating-coal usage were taken into account (Zhai *et al.*, 2019; Li *et al.*, 2020a, b). Industrial coal combustion during the PHS was an important source of trace elements. The TEO contents during the HS and PHS were much lower than 7.2% in Shijiazhuang in 2016, which indicated the efficiency of the CTG-derived energy switch (Lang *et al.*, 2018).

Fig. 5 shows the concentrations of metals and their rates of increase in the HP compared with the PHS. Increases in As and Cr by 65.1% and 20.4% in the HS, respectively led to an elevation in CRs. Again, Cd, Co, Pb, Rb, and Tl were enhanced by 147%, 18.7%, 152%, 77.8%, and 110%, respectively. Former studies have indicated that the above-mentioned metals are all markers of coal combustion, proving the increased coal usage in the HS (Tao *et al.*, 2014; Cui *et al.*, 2019; Li *et al.*, 2021a). It should be mentioned that Ba is as high as 2240 and 326 ng m^{-3} in the PHS and HS, and the reduction in the HS resulted in a decrease in TEO. Cu, Zn, and Pb were enhanced in the HS by 31.3%, 87.4%, and 152%, respectively, which indicated an increase in the mass contribution of vehicle exhaust to total $PM_{2.5}$ (Tao *et al.*, 2014; Xu *et al.*, 2019). Meanwhile, Al, Ca, Mg, and Fe decreased by 21.7%, 12.7%, 16.2%, and 23.7% in the HS compared with the PHS, which was attributed to the emissions control on dust and industries including iron, steel, and cement (Si *et al.*, 2021). V and Ni reduced by 1.92% and 56.2% in the HS, respectively, indicating emission reductions from oil-burning-related industries (Cui *et al.*, 2019). The smaller decrease in V as compared to Ni may have been a result of increased emissions from vehicles (Si *et al.*, 2021).

3.4 Health Risk Assessment and Concentrations of Heavy Metals

The carcinogenic risks (CRs) posed by inhalation of As, Cd, Cr(VI), Ni, Pb, and Co, and non-carcinogenic risks due to inhalation of As, Cr, Ni, Pb, Co, Fe, Cu, Zn, Cd, Sb, Mn, Sr, Sn, Ba, and Tl are shown in Fig. 6 and Tables S3–S6. Cr(VI) and As dominated in the CRs for children and adults in both the PHS and HS. The CRs to children caused by Cr(VI) were 5.32×10^{-6} and 6.40×10^{-6} in PHS and HS, and the corresponding values for adults were 2.13×10^{-5} and 2.56×10^{-5}, respectively. Cr(VI) comprised 80.5% and 77.8% in the total CRs for children, and 80.7% and 77.8% for adults,

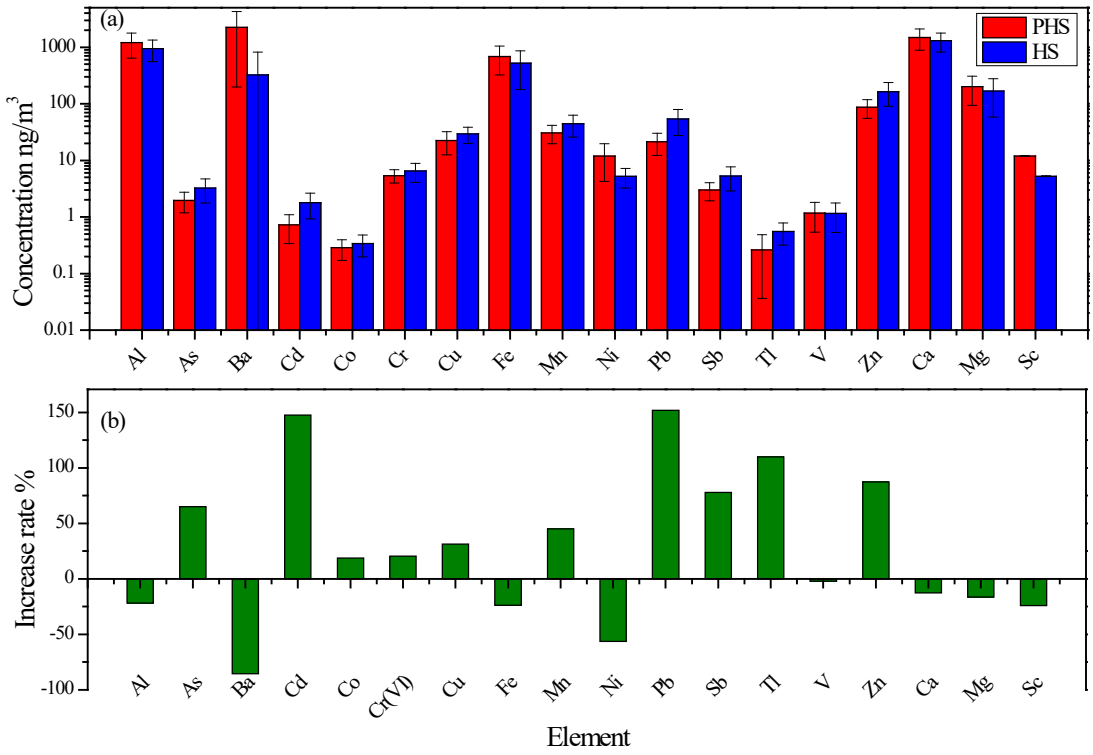

Fig. 5. (a) Concentrations of heavy metals and (b) their increase rates in the heating season as compared to the non-heating season.

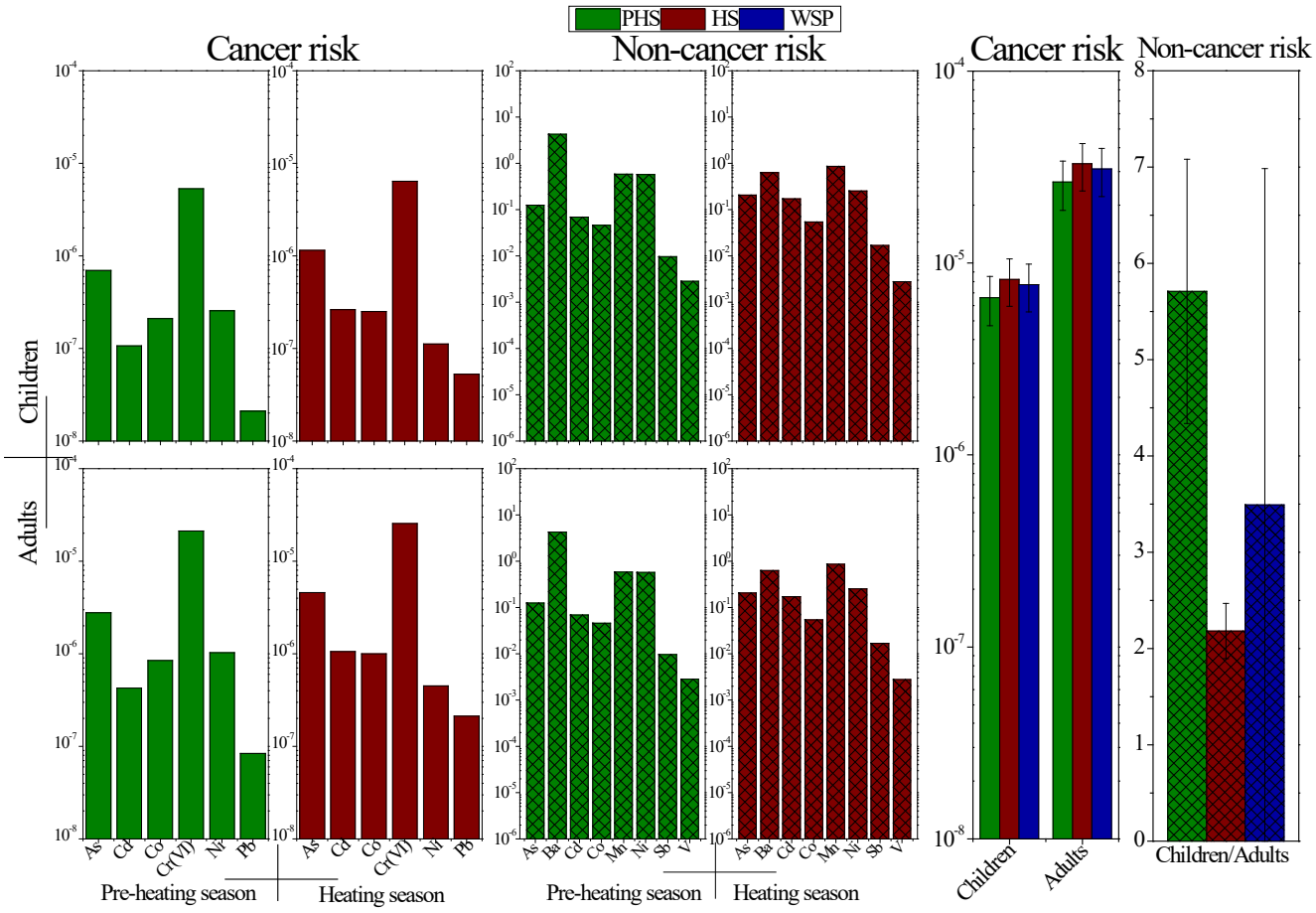

Fig. 6. Carcinogenic and non-carcinogenic risks posed by $PM_{2.5}$ associated elements via inhalation.4

in the PHS and HS, respectively. From the PHS to the HS, the total CRs increased significantly from 6.61×10^{-6} to 8.23×10^{-6} and 2.64×10^{-5} to 3.29×10^{-5} for children and adults, respectively. The significant increase in the CRs in the HS were attributed to increased use of coal for heating.

Compared with Baoding in recent winters, the total CRs for children in the HS in this study were higher than 7.6×10^{-6} in 2017, and lower than 1.18×10^{-5} in 2016 without implementation of clean heating (Si *et al.*, 2021). The total CRs for adults in the HS showed similar trends, where the 3.29×10^{-5} in 2019 was higher than the 3.15×10^{-5} in 2017 and much lower than the 4.87×10^{-5} in 2016. This was in accordance with the fact that coal usage decreased due to the strict coal banning law passed in 2017, which was not in place in 2016. However, while increased again in 2019 due to a lack of enforcement of the coal-banning policy (Zhai *et al.*, 2019).

Unlike CRs, a reverse trend was found for non-carcinogenic risks (NCRs) represented by the total hazard quotients (HQs) (Fig. 6). The total HQs in the entire sampling period (ESP) was 3.49 ± 0.89 and exceeded the accept level of one, which should be given more attention by the local government. The total HQs decreased from 5.71 in the PHS to 2.18 in the HS, indicating the impact of an obvious reduction in Ba. It should be noted that the mass concentration of Ba was as high as 2240 in the PHS and 326 ng m^{-3} in the HS, which was far higher than the 41.3 and 18.2 ng m^{-3} in 2016 and 2017, respectively (Fig. 7). In addition to natural sources, glass production is a key emission source of Ba (Cui *et al.*, 2019; Xu *et al.*, 2019; Si *et al.*, 2021). The extremely high Ba concentration could have been due to a local large-scale glass production factory. The backward trajectory analysis provided support for this assumption, which is discussed in detail in Section 3.6. The significantly reduced Ba in the HS by 85.5% relative to the PHS was closely related to the production stoppages/limitations and staggered peak production in the glass industry.

3.5 Source Apportionment by PMF

Fig. S2 shows the source profiles for seven recognized emission sources using the PMF model. Factor 1 was mainly composed by NH_4^+, NO_3^-, and SO_4^{2-}, which was attributed to secondary inorganic aerosols (SIA) (Si *et al.*, 2021). These secondary products were formed by the oxidation of precursor gases including SO_2 and NO_x released mainly from the coal/biomass/natural gas combustion, automobile exhaust, and industrial processes, which in turn reacted with NH_3 derived from agricultural activities and livestock waste (Tao *et al.*, 2014; Cui *et al.*, 2019; Xu *et al.*, 2019).

Factor 2 was represented by a high load of Cu, Zn, Ca^{2+}, Mg^{2+}, and specific levels of Pb and Cd. Cu and Zn have been demonstrated to be good markers of VE (Xu *et al.*, 2019). Cu is found in brake systems, and Zn and Pb are found in automobile exhaust (Cui *et al.*, 2019). Cd is an important element in lubricants and tires (Xu *et al.*, 2019; Zhang *et al.*, 2018). Ca^{2+} and $Mg^{2+}$are often used as road dust indicators (Cui *et al.*, 2019).

Factor 3 was identified as fugitive dust (FD) characterized by high loadings of crustal elements such as Al, Mg, Si, Ca, Ti, and Fe (Si *et al.*, 2021). Suspended dust often comes from dust accumulated due to wind on unpaved roads, construction sites, and bare soil around cities (Tao *et al.*, 2014).

High fractions of Cl^- and K^+ presented in factor 4, which was attributed to biomass burning (Tao *et al.*, 2014; Feng *et al.*, 2018; Zhai *et al.*, 2019). K^+ and Cl^- have been commonly used to identify wood burning activities and agricultural residues (Feng *et al.*, 2018).

Factor 5 possessed high loadings of a host of trace metals including Cd, Mn, Pb, Tl, Ag, Fe, Ni, V, Zn, Cu, and Cr, indicating industrial emissions. Zn, Cd, Pb, Tl, and Ag often originate from waste incineration (Cui *et al.*, 2019; Si *et al.*, 2021). V, Cr, and Ni are closely related to oil combustion (Xu *et al.*, 2019). Cu, Zn, and Ag are widely used in electroplating processes (Si *et al.*, 2021). Fe and Cr are markers for iron-steel production (Xu *et al.*, 2019). The above-mentioned industries are clustered in Baoding and adjacent counties.

Factor 6 represents high contributions of As, SO_4^{2-}, and Cl^-, along with moderate loadings of Pb, Cu, Zn, Sn, Pb, Tl, and Sb was found in this factor, which were attributed to coal combustion (Tao *et al.*, 2014; Li *et al.*, 2021a). Zhao *et al.* (2020a) ascribed the high Pb and Zn in winter $PM_{2.5}$ observed in Beijing to coal combustion. Factor 7 was characterized by the highest load of Ba (85.7%), which was identified as due to glass production (Cui *et al.*, 2019; Xu *et al.*, 2019). Fuyao Glass Co., Ltd. is located 15 kilometers northwest of Baoding City, which supports this supposition.

Time series of source contributions for each sampling day and the averaged contributions in the PHS, HS, and ESP are shown in Fig. 7. In the case of ESP, fugitive dust (FD) and vehicle emissions (VE)

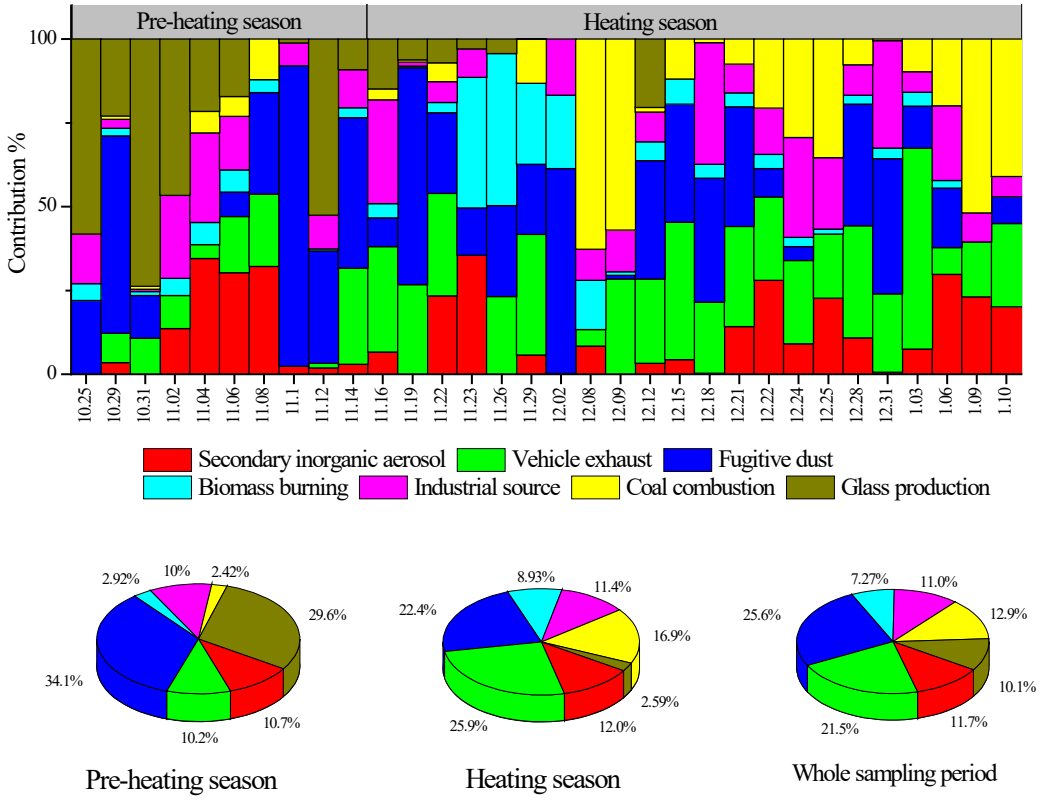

Fig. 7. Contributions of seven sources to the $PM_{2.5}$ mass.

were the top contributors, contributing 25.6% and 21.5% to the $PM_{2.5}$ mass, respectively. The highest fractions of FD and VE further evidenced effective emission reductions on the part of industries, as well as coal/biomass combustion. Table 1 lists the results of source contributions recently obtained using a PMF model in China. The coal combustion (CC) fraction of 12.9% obtained in this study was much lower than the previously reported 34.8% in 2014, 49% in the winter of 2015, and 22.6% in 2016 for Baoding, indicating effective prohibition of coal utilization. Also, this figure was far lower than the 43% found for the adjacent urban site of Wangdu County in the winter of 2015 and the 58% and 40.5% at a rural site in Wangdu County in the winter of 2015 and 2017, respectively. Among large cities, Beijing and Tianjin had declining CC fractions, indicating adherence to the strict coal banning law. A CC fraction of 12.9% in Baoding in 2019 was still higher than the 8.8% found for Beijing in the winter of 2017 and the 10% for Tianjin in 2016, illustrating a gap in the enforcement of the coal ban in large and small cities (Zhai *et al.*, 2019). A biomass burning (BB) fraction of 7.27% for Baoding in 2019 was lower than the 12% and 8.7% of Beijing in 2001–2004 and 2012–2013 and the 10.2% in Tianjin in the winter of 2015, implying the impact of the biomass-burning prohibition in Baoding. However, it was higher than the 4.1% in Beijing in the winter of 2017 and the 5.3% in Tianjin from 2014–2015, indicating that biomass-burning should be further managed. After stopped/limited/staggered production and the adoption of advanced emissions control devices and techniques, the industrial sources (IS) fraction in Baoding was much lower than the 13.2% in Baoding and the 20.5% in Shijiazhuang in 2016. It should be noted that glass production had become an important source, which contributed a $PM_{2.5}$ mass of 10.1% after effective control of iron-steel production and electroplating. The FD fraction for Baoding in the ESP was higher than most reported values for Beijing, Tianjin, and Shijiazhuang, indicating that there were impacts of emission reductions on CC, BB, and IS. The high FD fraction in Baoding City suggested that control of FD must be strengthened.

Obvious variations between the PHS and HS in terms of source contributions were found in Baoding (Fig. 7). The CC contributions increased significantly from 2.42% in the PHS to 16.9% in the HS, which was mainly attributed to the coal combustion used for indoor heating. Again, the BB fractions increased from 2.92% in the PHS to 8.93% in the HS, indicating that adjacent rural

Table 1. Comparisons of source contributions of $PM_{2.5}$ among different regions in China.

Site	Date	SIA	BB	CC	IS	VE	FD	GP	References
BD (urban)	Winter, 2019	11.7	7.27	12.9	11.0	21.5	25.6	10.1	This study
BJ (urban)	Winter, 2015	-	-	32	-	-	-	-	Liu *et al.* (2017b)
BJ (urban)	Winter, 2017	37.7	4.1	8.8	7.9	21.3	9.0	-	Huang *et al.* (2021)
BD (urban)	2014	9.7	-	34.8	-	14	16.9	-	Gao *et al.* (2018)
BD (urban)	Winter, 2015	-	-	49	-	-	-	-	Liu *et al.* (2017a)
BD (urban)	2016	38.1	-	22.6	13.2	10.2	8.7	-	Xu *et al.* (2019)
WD (urban)	Winter, 2015	-	-	43	-	-	-	-	Liu *et al.* (2017b)
DBT (rural)	Winter, 2015	-	-	58	-	-	-	-	Liu *et al.* (2017b)
DBT (rural)	Winter, 2017	21.2	16.4	40.5	-	10.8	8.6	-	Zhao *et al.* (2020b)
TJ (urban)	2014	13.1	-	25.6	-	23.5	26.4	-	Gao *et al.* (2018)
TJ (urban)	2014–2015	29.2	5.3	12.4	-	15.2	11.7	-	Huang *et al.* (2017)
TJ (urban)	Summer, 2015	26.1	10.2	16.5	-	25.4	25.4	-	Liu *et al.* (2017a)
TJ (urban)	2016	40.6	0	10	10.4	17.4	10.1	-	Xu *et al.* (2019)
SJZ (urban)	2016	39.1	-	18.3	20.5	11	8	-	Xu *et al.* (2019)
CZ (urban)	2016	39.1	-	17.1	10.7	11.9	16.7	-	Xu *et al.* (2019)

residents preferred using biomass as heating fuel due to lower costs (Zhao *et al.*, 2020a, b). VE also increased from 10.2% to 25.9%, which was a result of the citizens' willingness to drive in cold weather. Therefore, CC, BB, and VE should be further managed. It is worth mentioning that the contribution of glass production (GP) decreased significantly from 29.6% in the PHS to 2.59% in the HS by 91.3%, demonstrating emission reductions on the part of large-size enterprises.

3.6 Backward Trajectory Clustering

Fig. S3 shows the origins of air masses in Baoding City in the PHS, HS and ESP. A total of four trajectories were clustered for three periods. No significant differences in air mass origins were found between the PHS and HS. In the HS, 27.4% and 24.1% of the trajectories were derived from Northwest Mongolia and Russia; 20.5% were derived from west Inner Mongolia and Shanxi Province, and 27.6% were derived from Beijing. The dust from Northwest Mongolia, Russia, and Inner Mongolia may have increased the FD fraction in Baoding. The 100% CTG penetration rate in Beijing may have been the source of NO_3^- in addition to the large amounts of SNN generated by local heating (Zhao *et al.*, 2020a). It should be noted that 74.3% of the trajectories from the northwest flowed through the Xushui District in Baoding where a large glass-making factory is located, which caused increases in related pollutants, especially Ba.

4 CONCLUSIONS

A field observation was conducted in Baoding in 2019, covering the pre-heating season (PHS) and the heating season (HS) in order to evaluate the impacts of "clean heating."

1) On average, $PM_{2.5}$ concentrations increased from 69.1 in the PHS to 129 μg m^{-3} in the HS.
2) In the HS, higher increases in the rates SO_4^{2-} by 270% as compared to 109% of NO_3^- supported a premise of higher coal combustion (CC) for heating purposes. Also, the NO_3^-/SO_4^{2-} ratio decreased from 2.75 in the PHS to 2.08 in the HS, and CC markers, As, Rb, and Tl, increased by 65.1%, 77.8%, and 110%, respectively.
3) The reduced Al, Ca, Mg, and Fe, V, and Ni in the HS indicated effective control of dust and the iron-steel/cement/oil-burning industries. The total carcinogenic risks increased significantly in the HS due to the elevated As and Cr. In contrast, the HS had fewer non-carcinogenic risks due to the reduced Ba.
4) The contributions of CC and biomass burning led to significant increases of 598% and 206%, respectively, indicating they were still serious in spite of the coal/biomass banning law. It should be noted that the contribution of glass production was prominent, marked by Ba as high as 2240 and 326 ng m^{-3} in the PHS and HS, respectively.

It is suggested that increasing the penetration rate of "coal to gas", reducing the emissions from

glass production, and installing the de-NOx equipment for natural gas burning enterprises should be strengthened to further improve air quality in the heating season.

ACKNOWLEDGEMENTS

This study was supported by the Beijing Natural Science Foundation of (8212034), the Natural Science Foundation of Hebei Province (B2020502007), the Fundamental Research Funds for the Central Universities (2020MS125), the Science and Technology Projects of Baoding (2141ZF321), and the "Three Three Three Talent Project" of Hebei Province (A202001055).

SUPPLEMENTARY MATERIAL

Supplementary material for this article can be found in the online version at https://doi.org/10.4209/aaqr.210333

REFFERENCES

Carter, E., Yan, L., Fu, Y., Robinson, B., Kelly, F., Elliott, P., Wu, Y.F., Zhao, L.C., Ezzati, P., Yang, X.D., Chan, Q., Baumgartner, J. (2020). Household transitions to clean energy in a multiprovincial cohort study in China. Nat. Sustain. 3, 42–50. http://doi.org/10.1038/s41893-019-0432-x

Chen, Z.Y., Chen, D.L., Wen, W., Zhuang, Y., Kwan, M.P., Chen, B., Zhao, B., Yang, L., Gao, B.B., Li, R., Xu, B. (2019). Evaluating the "2+26" regional strategy for air quality improvement during two air pollution alerts in Beijing: variations in $PM_{2.5}$ concentrations, source apportionment, and the relative contribution of local emission and regional transport. Atmos. Chem. Phys. 19, 6879–6891. https://doi.org/10.5194/acp-19-6879-2019

Cheng, J., Su, J., Cui, T., Li, X., Dong, X., Sun, F., Yang, Y., Tong, D., Zheng, Y., Li, Y., Li, J., Zhang, Q., He, K. (2019). Dominant role of emission reduction in $PM_{2.5}$ air quality improvement in Beijing during 2013–2017: A model-based decomposition analysis, Atmos. Chem. Phys. 19, 6125–6146. https://doi.org/10.5194/acp-2018-1145

Cui, Y., Ji, D., Chen, H., Gao, M., Maenhaut, W., He, J., Wang, Y. (2019). Characteristics and sources of hourly trace elements in airborne fine particles in urban Beijing, China. J. Geophys. Res. 124, 11595–11613. http://doi.org/10.1029/2019jd030881

Feng, J., Yu, H., Mi, K., Su, X., Li, Y., Li, Q., Sun, J. (2018). One year study of $PM_{2.5}$ in Xinxiang City, north China: Seasonal characteristics, climate impact and source. Ecotoxicol. Environ. Saf. 154, 75–83. https://doi.org/10.1016/j.ecoenv.2018.01.048

Gao, J.J., Wang, K.,Wang, Y.,Liu, S.H.,Zhu, C.Y.,Hao, J.M., Liu, H.J., Hua, S.B., Tian, H.Z. (2018). Temporal-spatial characteristics and source apportionment of $PM_{2.5}$ as well as its associated chemical species in the Beijing-Tianjin-Hebei region of China. Environ. Pollut. 233, 714–724. https://doi.org/10.1016/j.envpol.2017.10.123

Hu, X., Zhang, Y., Ding, Z., Wang, T., Lian, H., Sun, Y., Wu, J. (2012). Bioaccessibility and health risk of arsenic and heavy metals (Cd, Co, Cr, Cu, Ni, Pb, Zn and Mn) in TSP and $PM_{2.5}$ in Nanjing, China. Atmos. Environ. 57, 146–152. http://doi.org/10.1016/j.atmosenv.2012.04.056

Huang, X., Liu, Z.R., Liu, J.Y., Hu, B., Wen, T.X., Tang, G.Q., Zhang, J.K., Wu, F.K., Ji, D.S., Wang, L.L. (2017). Chemical characterization and source identification of $PM_{2.5}$ at multiple sites in the Beijing-Tianjin-Hebei region, China. Atmos. Chem. Phys. 17, 1241–12962. https://doi.org/10.5194/acp-17-12941-2017

Huang, X.J., Tang, G.Q., Zhang, J.K., Liu, B.X., Liu, C., Zhang, J., Cong, L.L., Cheng, M.T., Yan, G.X., Gao, W.K., Wang, Y.H., Wang. Y.S. (2021). Characteristics of $PM_{2.5}$ pollution in Beijing after the improvement of air quality. J. Environ. Sci. 100, 1–10. https://doi.org/10.1016/j.jes.2020.06.004

Lang, J.L., Li, S.Y., Cheng, S.Y., Zhou, Y., Chen, D.S., Zhang, Y.Y., Zhang, H.Y., Wang, H.Y. (2018). Chemical characteristics and sources of submicron particles in a city with heavy pollution in China. Atmosphere 9, 388–407. https://doi.org/10.3390/atmos9100388

Li, Z.Y., Guo, S.T., Li, Z.X., Wang, Y.T., Hu, Y., Xing, Y.R., Liu, G.Q., Fang, R., Zhu, H.T. (2020a). $PM_{2.5}$ associated phenols, phthalates, and water-soluble ions from five stationary combustion

sources. Aerosol Air Qual. Res. 20, 61–71. https://doi.org/10.4209/aaqr.2019.11.0602

Li, Z.Y., Wang, Y.T., Li, Z.X., Guo, S.T., Hu, Y. (2020b). Levels and sources of $PM_{2.5}$-associated PAHs during and after the wheat harvest in a central rural area of the Beijing-Tianjin-Hebei (BTH) region. Aerosol Air Qual. Res. 20, 1070–1082. https://doi.org/10.4209/aaqr.2020.03.0083

Li, Z.Y., Li, Z.X., Yue, Z.Y., Yang, D.Y., Wang, Y.T., Chen, L., Guo, S.T., Yao, J.S., Wang, L., Lou, X., Xu, X.L., Wei, J.Y., Deng, B.L., Wu, H. (2021a). Impact of wheat harvest on levels and sources of $PM_{2.5}$-associated PAHs in an urban area located at the center of Beijing-Tianjin-Hebei region. Aerosol Air Qual. Res. 21, 200625. https://doi.org/10.4209/aaqr.200625

Li, Z.Y., Yue, Z.Y., Yang, D.Y., Wang, L., Wang, X., Li, Z.X., Wang, Y.T., Chen, L., Guo, S.T., Yao, J.S., Lou, X., Xu, X.L., Wei, J.Y. (2021b). Levels, chemical compositions, and sources of $PM_{2.5}$ of rural and urban area under the impact of wheat harvest. Aerosol Air Qual. Res. 21, 210026. https://doi.org/10.4209/aaqr.210026

Liu, B.S., Yang, J.M., Yuan, J., Wang, J., Dai, Q.L., Li, T.K., Bi, X.H., Feng, Y.C., Xiao, Z.M., Zhang, Y.F., Xu, H. (2017a). Source apportionment of atmospheric pollutants based on the online data by using PMF and ME2 models at a megacity, China. Atmos. Res. 185, 22–31. https://doi.org/10.1016/j.atmosres.2016.10.023

Liu, P.F., Zhang, C.L., Xue, C.Y., Mu, Y.J., Liu, J.F., Zhang, Y.Y., Tian, D., Ye, C., Zhang, H.X., Guan, J. (2017b). The contribution of residential coal combustion to atmospheric $PM_{2.5}$ in Northern China during winter. Atmos. Chem. Phys. 17, 11503–11520. https://doi.org/10.5194/acp-2017-281

Megido, L., Suarez-Pena, B., Negral, L., Castrillon, L., Fernandez-Nava, Y. (2017). Suburban air quality: Human health hazard assessment of potentially toxic elements in PM_{10}. Chemosphere 177, 284–291. https://doi.org/10.1016/j.chemosphere.2017.03.009

Pang, N.N., Gao, J., Chen, F., Ma, T., Liu, S., Yang, Y., Zhao, P.S., Yuan, J., Liu, J.Y., Xu, Z.J. (2020). Cause of $PM_{2.5}$ pollution during the 2016-2017 heating season in Beijing, Tianjin, and Langfang, China. J. Environ. Sci. 95, 201–209. https://doi.org/10.1016/j.jes.2020.03.024

Pozzer, A., Schultz, M.G., Helmig, D. (2020). Impact of U.S. oil and natural gas emission increases on surface ozone is most pronounced in the central United States. Environ. Sci. Technol. 54, 12423–12433. https://doi.org/10.1021/acs.est.9b06983

Si, R., Xin, J., Zhang, W., Wen, T., Li, S., Ma, Y., Wu, X., Cao, Y., Xu, X., Tang, H., Xu, J., Li, X., Wang, Y., Wu, F. (2021). Environmental and health benefits of establishing a coal banning area in the Beijing-Tianjin-Hebei Region of China. Atmos. Environ. 247, 118191. https://doi.org/10.1016/j.atmosenv.2021.118191

Tao, J., Gao, J., Zhang, L., Zhang, R., Che, H., Zhang, Z., Lin, Z., Jing, J., Cao, J., Hsu, S.C. (2014). $PM_{2.5}$ pollution in a megacity of southwest China: Source apportionment and implication. Atmos. Chem. Phys. 14, 8679–8699. https://doi.org/10.5194/acp-14-8679-2014

Wang, Y.T., Zhang, Y., Li, X., Cao, J.J. (2021). Refined source apportionment of atmospheric $PM_{2.5}$ in a typical city in northwest China. Aerosol Air Qual. Res. 21, 200146. https://doi.org/10.4209/aaqr.2020.04.0146

Xu, H., Xiao, Z., Chen, K., Tang, M., Zheng, N.Y., Li, P., Yang, N., Yang, W., Deng, X.W. (2019). Spatial and temporal distribution, chemical characteristics, and sources of ambient particulate matter in the Beijing-Tianjin-Hebei region. Sci. Total Environ. 658, 280–293. https://doi.org/10.1016/j.scitotenv.2018.12.164

Yao, L., Yang, L.X., Yuan, Q., Yan, C., Dong, C., Meng, C.P., Sui, X., Yang, F., Lu, Y.L., Wang, W.X. (2016). Source apportionment of $PM_{2.5}$ in a background site in the North China Plain. Sci. Total Environ. 541, 590–598. https://doi.org/10.1016/j.scitotenv.2015.09.123

Zhai, S.X., Jacob, D.J., Wang, X., Shen, L., Li, K., Zhang, Y.Z., Gui, K., Zhao, T.L., Liao, H. (2019). Fine particulate matter ($PM_{2.5}$) trends in China, 2013-2018: Separating contributions from anthropogenic emissions and meteorology. Atmos. Chem. Phys. 19, 11031–11041. https://doi.org/10.5194/acp-19-11031-2019

Zhang, Y., Lang, J., Cheng, S., Li, S., Zhou, Y., Chen, D., Zhang, H., Wang, H. (2018). Chemical composition and sources of PM_1 and $PM_{2.5}$ in Beijing in Autumn. Sci. Total Environ. 630, 72–82. https://doi.org/10.1016/j.scitotenv.2018.02.151

Zhao, S.M., Hu, B., Gao, W.K., Li, L.C., Huang, W., Wang, L.L., Yang, Y., Liu, J.D. Li, J.Y., Ji, D.S., Zhang, R.J., Zhang, Y.Y., Wang, Y.S. (2020a). Effect of the "coal to gas" project on atmospheric NO_x during the heating period at a suburban site between Beijing and Tianjin. Atmos. Res. 241, 104977. https://doi.org/10.1016/j.atmosres.2020.104977

Zhao, X.X., Zhao, X.J., Liu, P.F., Ye, C., Xue, C.Y., Zhang, C.L., Zhang, Y.Y., Liu, C.T., Liu, J.F., Chen, H., Chen, J.M., Mu, Y.J. (2020b). Pollution levels, composition characteristics and sources of atmospheric $PM_{2.5}$ in rural area of the North China Plain during winter. J. Environ. Sci. 95, 172–182. http://doi.org/10.1016/10.1016/j.jes.2020.03.053

Zheng, B., Tong, D., Li, M., Liu, F., Hong, C.P., Geng, G.N., Li, H.Y., Li, X., Peng, L.Q., Qi, J., Yan, L., Zhang, Y.X., Zhao, H.Y., Zheng, Y.X., He, K.B., Zhang, Q. (2018). Trends in China's anthropogenic emissions since 2010 as the consequence of clean air actions. Atmos. Chem. Phys. 18, 14095–14111. https://doi.org/10.5194/acp-2018-374